

TREE-RING RECONSTRUCTION OF UPPER  
GILA RIVER DISCHARGE<sup>1</sup>*David Meko and Donald A. Graybill<sup>2</sup>*

**ABSTRACT:** Effective planning for use of water resources requires accurate information on hydrologic variability induced by climatic fluctuations. Tree-ring analysis is one method of extending our knowledge of hydrologic variability beyond the relatively short period covered by gaged streamflow records. In this paper, a network of recently developed tree-ring chronologies is used to reconstruct annual river discharge in the upper Gila River drainage in southeastern Arizona and southwestern Arizona since A.D. 1663. The need for data on hydrologic variability for this semi-arid basin is accentuated because water supply is inadequate to meet current demand. A reconstruction based on multiple linear regression ( $R^2=0.66$ ) indicates that 20th century is unusual for clustering of high-discharge years (early 1900s), severity of multiyear drought (1950s), and amplification of low-frequency discharge variations. Periods of low discharge recur at irregular intervals averaging about 20 years. Comparison with other tree-ring reconstructions shows that these low-flow periods are synchronous from the Gila Basin to the southern part of the Upper Colorado River Basin.

(**KEY TERMS:** surface water hydrology; tree rings; drought; Gila River; meteorology/climatology; modeling/statistics; history.)

## INTRODUCTION

The Upper Gila River Basin (UGRB) is the major source of surface water for southeastern Arizona and southwestern New Mexico. Surface water is inadequate for current demand and is the subject of litigation among water users (Gold and Denis, 1986). The supply is also uncertain because precipitation in this semiarid region varies greatly on time scales of decades and longer (Thomas, 1962). Water resources planning for such basins can benefit from accurate information on the range of variability of hydrologic parameters that might be expected from climatic

fluctuations. The period covered by gaged records supplies a single, relatively short sample with which to gage the variability. Tree rings have proved useful in diverse hydrologic regimes for inferring water-supply variability on long time scales (Loaiciga *et al.*, 1993). Tree-ring reconstructions for the Salt and Verde Rivers, Arizona, and for various rivers in the Upper Colorado River Basin indicate that multiyear hydrologic drought over the past 400 years has at times been much more severe than droughts sampled by gaged discharge records (e.g., Stockton and Jacoby, 1976; Smith and Stockton, 1981). Because of regional differences in climate variations, however, these results cannot be assumed to apply to the UGRB.

The UGRB differs from the Upper Colorado and Salt and Verde basins in its more southerly location and more dominant summer convective rainfall component. A pilot study using a few tree-ring sites in a small sub-basin of the UGRB showed that properly selected trees integrate moisture conditions over seasons such that tree-ring data retain a strong statistical signal for annual runoff (Stockton, 1975). Field collections between 1985 and 1987 have expanded the network of well-replicated tree-ring chronologies sampling the main runoff-producing regions in the UGRB. In this paper, we reconstruct the annual discharge of the Gila River since A.D. 1663 from these new tree-ring collections. We discuss time-series features of the reconstruction related to water supply, and compare low-frequency variations of the reconstruction with those of other tree-ring reconstructions for a regional perspective on discharge variations.

<sup>1</sup>Paper No. 94113 of the *Water Resources Bulletin*. Discussions are open until April 1, 1996.

<sup>2</sup>Respectively, Research Specialist and Dendrochronologist, Laboratory of Tree-Ring Research, University of Arizona, Tucson, Arizona 85721 (Donald A. Graybill is deceased).

## DISCHARGE DATA

The UGRB for the purposes of this study is defined as the watershed above gage 09448500, or "gage 4485," the Gila River at the head of Safford Valley, near Solomon, Arizona (Figure 1). The watershed encompasses 20,450 km<sup>2</sup> of mainly mountains and grassland in southeastern Arizona and southwestern New Mexico. The monthly distribution of precipitation is bimodal, with a summer primary maximum from convective storms and a winter secondary maximum from cyclonic storms (Burkham, 1970). Mean annual precipitation ranges from less than 10 inches in the Safford Valley to more than 20 inches in the mountains of western New Mexico; corresponding annual runoff ranges from less than 0.2 inches to more than 2 inches (Anderson and White, 1986; Gold and Denis, 1986). Runoff is highest from December-May, mainly because of rain at lower elevations in December-March, and snowmelt at higher elevations in April and May (Stockton, 1975).

Monthly discharge data for gages in the UGRB were obtained from the U.S. Geological Survey database (EarthInfo Inc., 1990). The record at gage 4485 is continuous back to water year 1915, except for a few missing monthly values in the 1930s (U.S. Geological Survey, 1970). We estimated missing values from records at other gages using the HEC-4 Monthly Streamflow Simulation computer program (U.S. Army Corps of Engineers, 1971) to build a continuous monthly discharge record back to 1911. Mean annual discharge for 1911-1990 is 334,569 acre-ft.

The accuracy of the discharge record for gage 4485 is rated "good," meaning that 95 percent of the daily discharge measurements are within 10 percent of the true discharge (U.S. Geological Survey, 1970). The Gila River above gage 4485 is unregulated by major reservoirs, but water is diverted for 17,500 acres of irrigation (Anderson and White, 1986; U.S. Geological Survey, 1980). Burkham (1970) found that the ratio of discharge at gage 4485 to precipitation in the basin has been stable over time, suggesting that changes in irrigation have not seriously distorted the discharge record as an indicator of natural runoff.

## TREE-RING DATA

The tree-ring data consist of nine ring-width chronologies for five species at sites collected between 1985 and 1987 close to runoff-producing areas (Figure 1; Table 1). Trees were sampled from well-drained slopes with thin soil cover whenever possible to maximize the effective moisture stress. Disturbance

signals that could mask or confound the climate response were avoided by sampling from open stands where competition for light, water and soil nutrient is low, and where tree growth had not been widely affected by fire or human activity, such as construction or logging. Specimens with injury from lightning or with obvious damage from disease or insects were avoided. Two increment cores (4.3 mm diameter) were normally taken transverse to the prevailing ground slope at breast height from opposing sides of each of 10-20 trees.

Tree rings were dated and measured using standard procedures (Cook and Kairiukstis, 1990). Biological growth trend was removed by fitting a negative exponential or straight line to each core's ring-width series, and dividing ring widths by corresponding values of the fitted line (Fritts, 1976). Information on monotonic trend in discharge over the full length of the tree-ring series is unavoidably removed by this operation.

Localized noise in the tree-ring data was reduced by averaging core indices over trees to form "site chronologies." Because most chronologies are significantly autocorrelated while annual discharge at gage 4485 is not, chronologies were prewhitened before use in regression by filtering with autoregressive-moving-average (ARMA) models. ARMA order was selected by the Akaike Information Criterion, and goodness of fit was evaluated with the "Q statistic," a measure of autocorrelation of residuals (Box and Jenkins, 1976). The residuals from the ARMA modeling are referred to as "residual" chronologies. Low-order models predominate in the ARMA fits (Table 2). The percentage of variance due to autocorrelation ranges from 2.6 percent to 29.5 percent. The original nine chronologies were reduced to six by combining residual chronologies from four species at Black Mountain, New Mexico, into a single Black Mountain chronology (site BKM in Figure 1).

Although core indices at several sites extend back before 1600, we have restricted our use of the data to the years after 1662 because of a sharp drop in sample size (number of trees) in earlier years. The likely detrimental effect of decreasing sample size on chronology variance is measured by the subsample signal strength *SSS*, a function of the sample size and the mean between-tree correlation of core indices (Wigley *et al.*, 1984). The percentage of climate variance explained in a reconstruction from a full-size chronology is multiplied by the factor *SSS* to get the expected variance explained from a reduced-size chronology. As shown in Table 2, *SSS* already exceeds 0.99 for some chronologies by 1663, and exceeds 0.95 for all except one chronology by 1800.

Tree-Ring Reconstruction of Upper Gila River Discharge

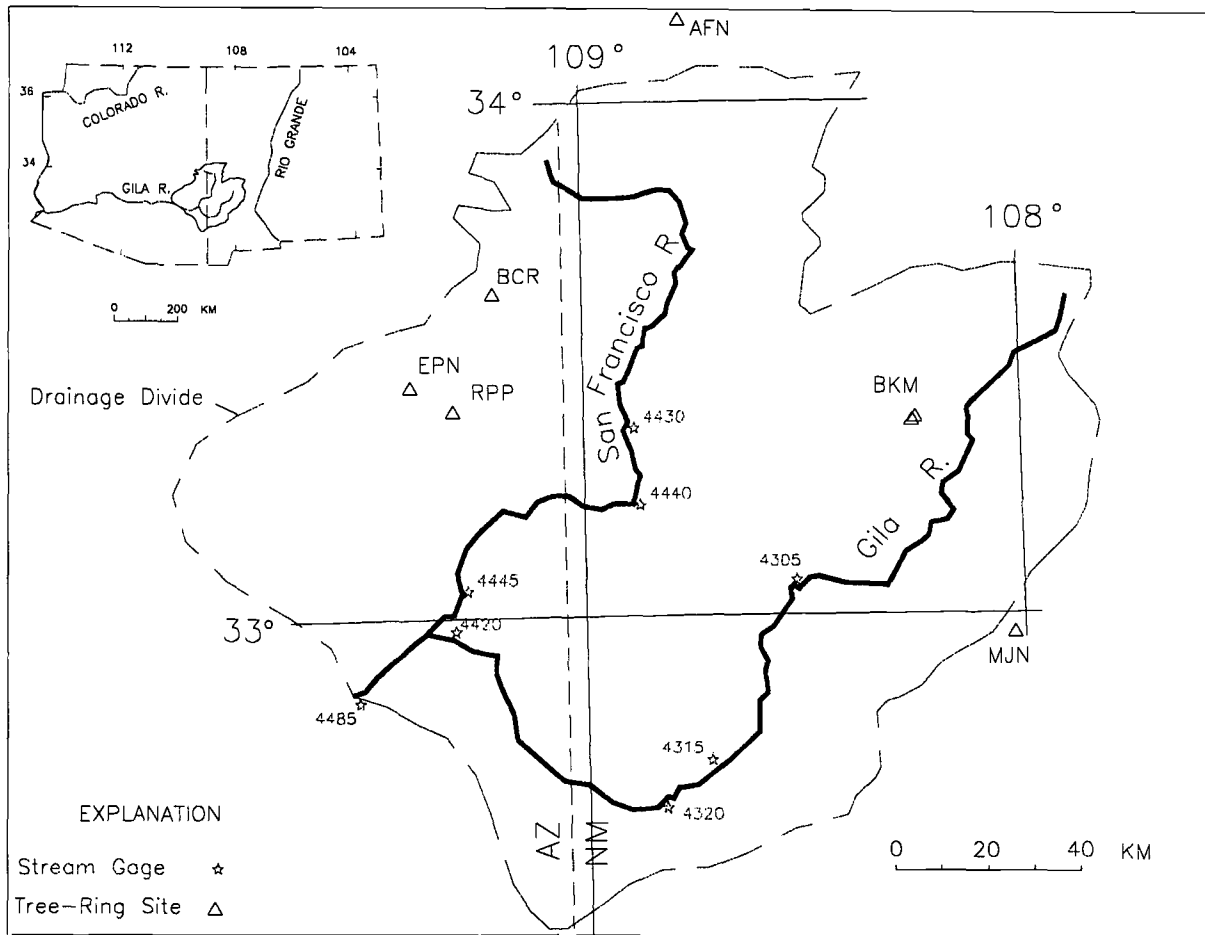


Figure 1. Map Showing the Boundary of the Gila River Drainage Above the Head of Safford Valley, Arizona, and Locations of Stream Gages and Tree-Ring Sites. Gage numbers are as in U.S. Geological Survey (1970), except that leading "09" and trailing "00" have been dropped. Four tree-ring sites are clustered at location "BKM".

TABLE 1. Site Information for Tree-Ring Chronologies.

Site	Code <sup>a</sup>	Spec <sup>b</sup>	Latitude	Longitude	Elevation (ft)
Agua Fria, New Mexico	AFN	pe	34°15'	108°37'	7220
Beaver Creek, Arizona	BCR	pp	33°42'	109°14'	7840
Black Mountain, New Mexico	BKM	pp,df,wp,wf	33°23'	108°14'	8400-9380
Eagle Creek, Arizona	EPN	pe	33°28'	109°29'	5540
Mimbres Junction, New Mexico	MJN	pe	32°57'	108°01'	6400
Rose Peak, Arizona	RPP	pp	33°25'	109°22'	7610

<sup>a</sup>Also used as map reference (Figure 1).

<sup>b</sup>Species coded as follows:

- pe = Pinyon pine (*Pinus edulis*)
- pp = Ponderosa pine (*Pinus ponderosa*)
- df = Douglas-fir (*Pseudotsuga menziesii*)
- wp = White pine (*Pinus strobiformis*)
- wf = White fir (*Abies concolor*)

TABLE 2. ARMA Models and Changes in Sample Size with Time for Chronologies.

Code <sup>a</sup>	ARMA Model <sup>b</sup>	ARMA Variance <sup>c</sup>	Sample Size <sup>d</sup> at Year				
			1663	1700	1800	1900	1985
AFN	(1,1)	9.7	8 <sup>#</sup>	16*	24*	24*	20*
BCR	(4,0)	4.5	10 <sup>#</sup>	24*	32*	32*	32*
BKA	(1,0)	2.6	1	3	13*	17*	23*
BKF	(1,1)	9.1	24*	24*	24*	24*	24*
BKP	(2,1)	22.9	14*	19*	22*	22*	22*
BKW	(1,1)	7.8	15*	17*	22*	20*	13*
BKM <sup>e</sup>	(1,1)	18.0	54*	63*	81*	83*	82*
EPN	(1,1)	4.3	2	4	9 <sup>#</sup>	29*	27*
MJN	(1,1)	11.7	4	8 <sup>#</sup>	21*	24*	23*
RPP	(1,1)	29.5	1	5	22*	22*	22*

<sup>a</sup>Site name coded as in Figure 1 and Table 1.

<sup>b</sup>Autoregressive-moving average model (p,q) with AR order p and MA order q fit to site chronology.

<sup>c</sup>Percentage of site chronology variance explained by ARMA model.

<sup>d</sup>Number of cores in site chronology at indicated year.

<sup>e</sup>Combined Black Mountain chronology.

<sup>#</sup>Subsample signal strength 95 percent.

\*Subsample signal strength 99 percent.

## RECONSTRUCTION MODEL

Exploratory data analysis indicated that the annual discharge series for gage 4485 was more skewed than the tree-ring chronologies, and that the relationships between the discharge series and the individual chronologies were strongly curvilinear. Log-transformed discharge was found to be approximately normally distributed and linearly related to the tree-ring series. A multiple linear regression model was developed to predict log-10 annual (water year) discharge from the residual chronologies described in the previous section. The log-10 discharge series was not prewhitened because none of its low-order autocorrelation coefficients (through lag 10) are significantly greater or less than zero at the 95 percent significance level (Box and Jenkins, 1976). The pool of potential predictors included 18 variables – the six residual chronologies lagged -1, 0, and +1 years from the water year of discharge.

Lagged predictors were included to allow the regression model to compensate for conceptual shortcomings of ARMA prewhitening as a filtering operation. Prewhitening tends to shift the autocorrelation structure of tree-ring data closer to that of annual discharge because tree-ring indices are typically more highly autocorrelated than annual discharge. The ARMA model cannot be expected, however, to be an optimal filter for converting a tree-ring series into a proxy indicator of a specific hydrologic variable, such as river discharge. An obvious shortcoming arises from differences in the timing of the water year and the diameter-growth year. For example, if diameter growth stops in July of water-year  $t$ , any subsequent

rainfall in the same water year can be reflected only in later years' rings. But the ARMA tree-ring residual in year  $t$  depends only on the sequence of rings up to and including year  $t$ . By including lagged predictors, we retain the flexibility to incorporate such carryover effects to the extent that they significantly increase the river-discharge variance explained by the regression model.

A "full-period" model was calibrated using data for 1916-85, and the model was verified using a split-sample procedure, following Snee (1977). Predictors were allowed to enter the model stepwise in an order determined by the F-level for reduction of residual error variance until adjusted- $R^2$  reached a maximum (Weisberg, 1985). The final reconstruction equation is

$$\hat{y}_t = \hat{b}_0 + \sum_{i=1}^p \hat{b}_i x_{t,i} \quad (1)$$

where  $\hat{y}_t$  is the estimated log-10 discharge in year  $t$ ,  $p$  is the number of predictors in the model,  $\hat{b}_0, \hat{b}_1, \dots, \hat{b}_p$  are the estimated regression constant and coefficients, and  $x_{t,i}$  is the  $i^{\text{th}}$  predictor, a residual chronology in year  $t, t-1$  or  $t+1$ .

Predictors and estimated regression coefficients for the full-period model represented by Equation (1) are listed in Table 3. The model has nine predictors ( $p=9$ ) and explains 66 percent of the variance of log-10 discharge in the 1916-85 calibration period. The six chronologies contribute to the reconstruction through current or lagged relationships. Signs of coefficients on four of the five lagged terms are positive, indicating that the regression equation acts predominantly

as a low-pass filter on the ARMA tree-ring residuals. Because the predictors are intercorrelated, physical interpretation of contrasting signs and differing magnitudes of the regression coefficients is unwise (Mosteller and Tukey, 1977). Model assumptions were checked by analysis of the residuals  $\hat{\epsilon}_t = y_t - \hat{y}_t$ , where  $y_t$  is the observed log-10 discharge. Diagnostic statistics and plots (not shown) show that the residuals are approximately normally distributed, not autocorrelated, and not correlated with the predicted values.

	$r^2$	<i>RE</i>
First Half	0.58	0.52
Second Half	0.64	0.61

The  $r^2$  values are highly significant (p-value<0.001), and the *RE* values compare favorably with those for other successful tree-ring reconstructions of hydrologic and climatological variables (e.g., Cleaveland and Stahle, 1989; Cleaveland and Duvick, 1992).

Because tree-ring reconstructions are often used to infer characteristics of extreme events, the verification data of Figure 2 were examined to test the ability of the reconstruction to correctly identify exceptional low-flow years and high-flow years over the period 1916-1985. Dry years and wet years in the observed and predicted data were first delineated as those values outside the 0.14 and 0.84 quantiles of the sample distribution for 1916-1985, as marked by the horizontal lines in Figure 2. These thresholds, which are somewhat arbitrary, mark off about 15 percent of the data as dry years or wet years. The circles in Figure 2 mark years classified as dry or wet in the observed series; the asterisks mark years simultaneously dry (or wet) in the observed and predicted series. The significance of the observed relationships was tested using the hypergeometric distribution, which gives the probability,  $P_h$ , that at least  $m$  successes are obtained in  $n$  trials from a finite population of size  $N$  containing  $k$  successes (Dracup and Kahya 1994). In the application to low-flow years,  $N=70$  is the number of years in the observed flow series;  $k=10$  is the number of dry years in the observed flow series;  $n=10$  is the number of dry years in the predicted flow series; and  $m=6$  is the number of cases in which dry years in the observed and predicted series coincide. The corresponding probability of obtaining  $m \geq 6$  by chance according to the hypergeometric distribution is  $P_h < 0.0001$ . The same test applied to the wet years also yields a probability  $P_h < 0.0001$  that the observed relationships occur by chance. These results indicate significant ability of the reconstruction to classify unusually dry and wet years. The relationships for the reconstruction may actually be stronger than indicated because the reconstruction equation is based on 70 years of calibration while the verification predictions analyzed above with the hypergeometric test are based on 35-year calibration periods.

### LONG-TERM RECONSTRUCTION

The reconstructed log-10 discharge, 1663-1985, is plotted in Figure 3, along with horizontal lines at the 0.1, 0.5, and 0.9 quantiles to facilitate comparison of

TABLE 3. Summary of Regression Equation (70-year calibration).

Step <sup>a</sup>	Site	Lag	$\hat{b}$ <sup>b</sup>	SE( $\hat{b}$ ) <sup>c</sup>	p-value <sup>d</sup>
5	AFN	-1	0.07993	0.06283	0.21
8	AFN	+1	0.13034	0.06964	0.07
6	BCR	+1	0.19560	0.11881	0.10
2	BKM	0	0.17562	0.09967	0.08
7	BKM	+1	-0.18371	0.08936	0.04
4	EPN	0	0.13153	0.08337	0.12
3	MJN	-1	0.13010	0.06747	0.06
1	MJN	0	0.19416	0.08671	0.03
9	RPP	0	0.14864	0.10599	0.17
	Constant		5.42140	0.02317	0.00

$R^2 = 0.66$  squared coefficient of multiple determination  
 $\sigma = 0.1876$  standard error of the estimate

<sup>a</sup>Order of entry into equation by partial-F test.

<sup>b</sup>Estimated regression coefficient.

<sup>c</sup>Standard error of  $\hat{b}$ .

<sup>d</sup>For testing null hypothesis  $\hat{b}=0$  against alternative  $\hat{b} \neq 0$ .

The split-sample verification consisted of calibrating the model on 1916-1950 and verifying on 1951-1985, then calibrating on 1951-1985 and verifying on 1916-1950. Regression  $R^2$  (variance explained) for the split samples is about the same as for the full-period model - 66 percent for the first half and 70 percent for the second.

The observed and predicted time series for the verification periods are plotted in Figure 2. The reconstruction appears to track year-to-year and decadal-scale fluctuations, reflect periods of persistent drought (e.g., 1950-1956), and respond to rapid reversals from wet to dry or from dry to wet conditions (e.g., 1917-1918 and 1918-1919). Verification accuracy was measured by the product-moment correlation coefficient ( $r^2$ ) and the reduction-of-error statistic (*RE*) (Cleaveland and Stahle, 1989). Values of these statistics for verifying on the first and second halves of the record are as follows:

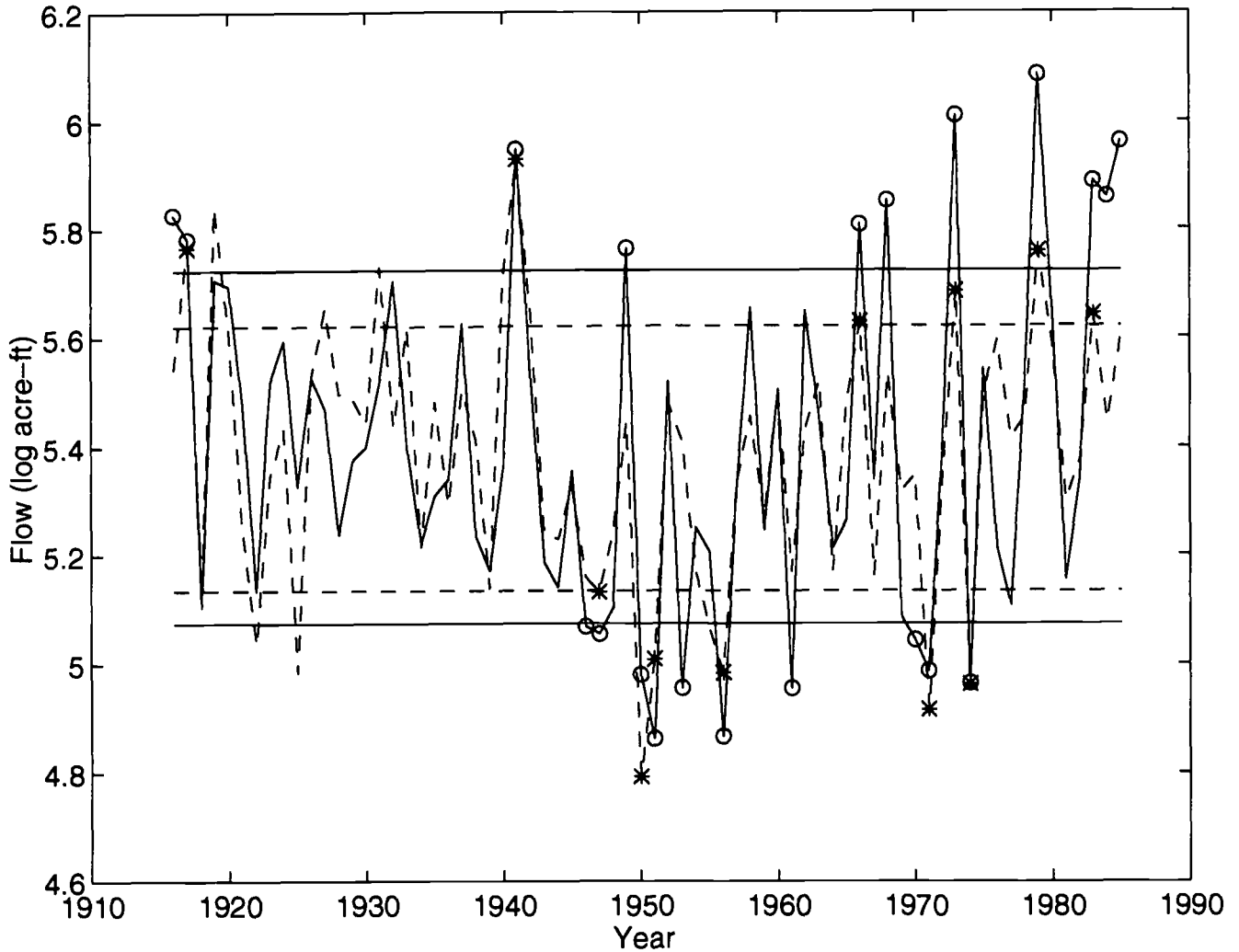


Figure 2. Time Series Plots, 1916-1985, of Observed Log-10 Discharge (solid) and Predictions Based on Split-Sample Verification Models (dashed). Horizontal lines mark the 0.14 and 0.84 quantiles of the plotted series. Values outside these quantiles are defined as dry or wet years, respectively. Dry years in the observed series are marked by circles; dry years in the reconstructed series that are also dry years in the observed series are marked by asterisks.

anomalies with normal conditions. The quantiles correspond to annual discharge of 125 KAF (thousand acre-ft), 272 KAF, and 503 KAF. The 20th century stands out for a period of recurrent high discharge about 1905-1915 and low discharge in the 1950s. The cluster of low-flow years in the 1950s coincides with a widespread meteorological drought whose temporal and spatial properties were charted by Thomas (1962). The sequence 1954-1956 was one of only two events with reconstructed discharge below the 0.1 quantile for three consecutive years. The other such event was 1818-1820, which contained the lowest annual reconstructed discharge value. The 1950s drought was in a sense more severe than the early-1800s drought, however, because the 1954-1956 sequence was imbedded within a broad period of

generally low discharge – including a two-year sequence below the 0.1 quantile in 1950-1951.

A conventional application of tree-ring data is to evaluate whether the modern gaged record is representative of the discharge history of the past few centuries. The period 1911-1985, during which the reconstruction overlaps gaged discharge records in the UGRB, is defined here as the “modern” period. Boxplots summarizing the frequency distributions of modern observed discharge and modern and long-term reconstructed discharge are shown in Figure 4. Medians and interquartile ranges transformed to volume-discharge units (KAF/yr) are also listed in Table 4.

Comparison of the two boxes for the modern period shows that the reconstructed median is biased high.

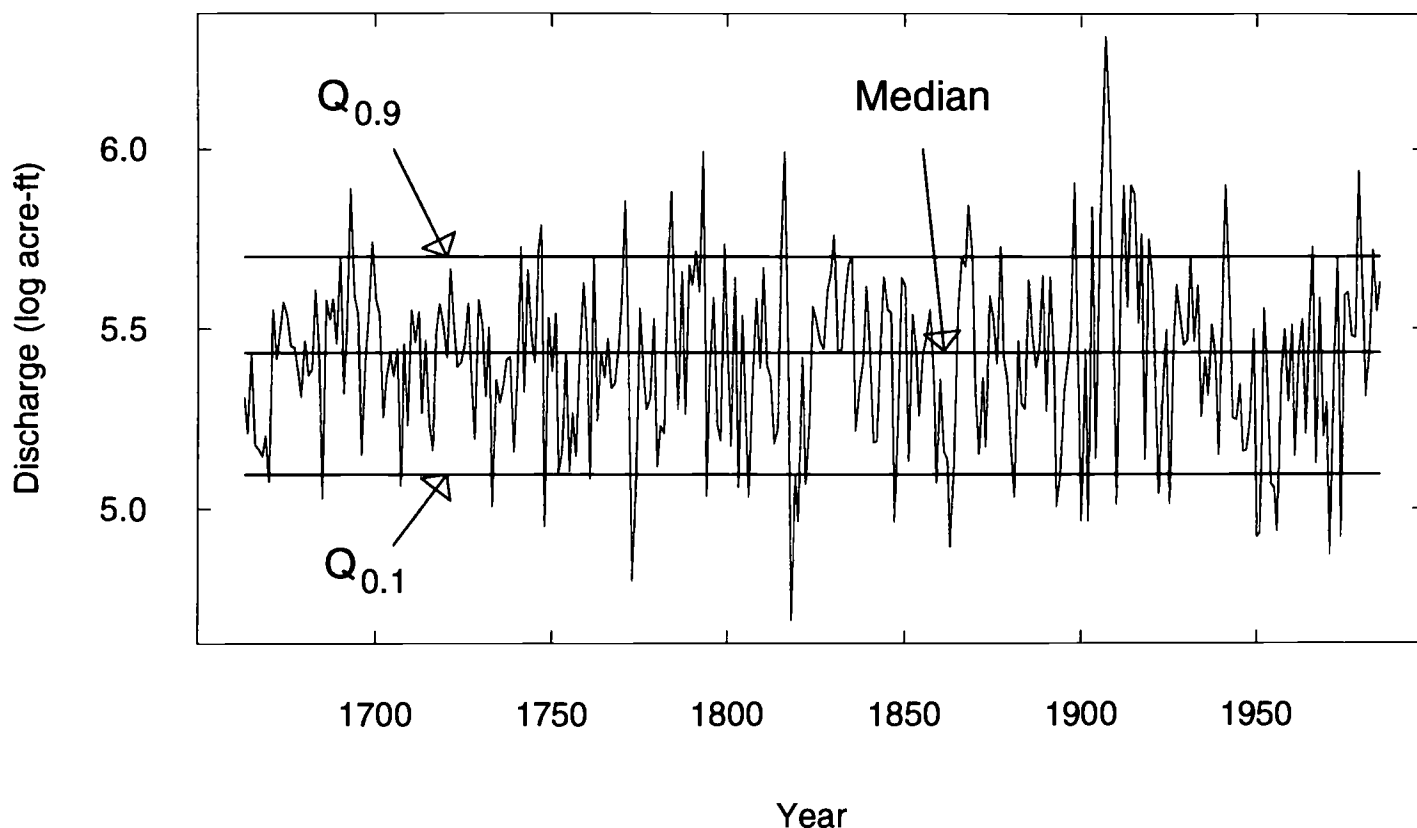


Figure 3. Time Series Plot of Reconstructed Gila River Discharge, 1663-1985. Horizontal lines are the 0.1, 0.5, and 0.9 quantiles.

Linear regression guarantees that the reconstructed mean for the calibration period (1916-1985) equals the observed mean, but does not constrain the median. As with regression estimates in general, the distribution of predicted values is compressed relative to that of the observed data. Comparison of the medians and interquartile ranges for reconstruction boxplots shows that the modern period is wet in a long-term context. The modern median is about 23 KAF above the long-term median of 272 KAF. The modern 75-year median ranks fifth highest of 249 medians computed for overlapping 75-year periods of the reconstruction.

The extremes in reconstructed annual discharge fall outside the modern period: the lowest value is in 1818, and the four highest values occur between 1905 and 1915. Variations in the frequency of extremely low and high discharge events were summarized by counting the number of years outside the 0.1 and 0.9 quantiles in each of 249 overlapping 75-year periods. These events are referred to as "dry years" and "wet years." The modern period has nine dry years and 10 wet years, slightly more than the median number (eight) for all 75-year periods. Earlier periods have

the highest frequencies of wet and dry years: several 75-year periods with start years between 1880 and 1900 have 12 dry years, and the period 1867-1941 has 15 wet years. Extreme events are rare in the early part of the reconstruction: several 75-year periods beginning in the 1600s had fewer than four dry years or wet years.

The persistence properties of hydrologic records are of particular interest in hydrologic planning for water supply. The lag-1 coefficient of the sample autocorrelation function (acf) of the the long-term reconstruction is 0.21, which for a sample size of 323 years is greater than zero at the 95 percent significance level. The acf of the full reconstruction at other lags (though lag 20) is essentially zero. The lag-1 coefficients of the acf for the 1916-1985 calibration period are 0.10 (observed log-10 discharge) and 0.13 (reconstruction), which are not significantly greater than zero for a sample size of 70 years. The reconstruction therefore suggests that short-term persistence is a characteristic of the flow series, a conclusion that could not be reached from analysis of the relatively short gaged record.

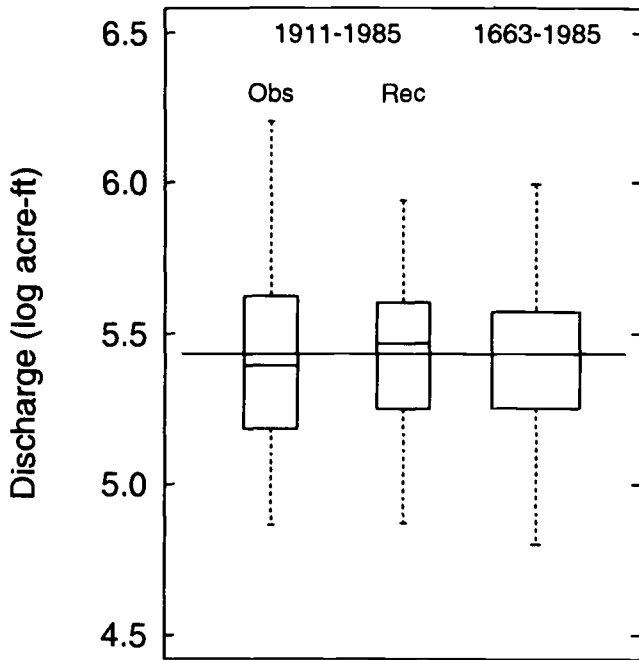


Figure 4. Boxplot Summaries of Frequency Distributions of Observed and Reconstructed Annual Log-10 Discharge. Left and central plots are for the 75-year modern period. Right plot is for full reconstruction. The boxplots mark the following quantities: median (horizontal line), interquartile range (box), range expected to contain 99.3 percent of the observations for a normally distributed variable (whiskers), and observations outside this range (dots). Whiskers are truncated at the data extremes if no observations fall outside the 99.3 percent range.

TABLE 4. Quantiles of Reconstructed and Observed Discharge.

Quantile	Annual Discharge (KAF)		
	Observed 1911-1985	Reconstructed	
		1911-1985	1663-1985
.75	422.3	401.9	374.8
.50	248.9	294.3	271.7
.25	153.4	178.8	179.9

A parameter of long-term persistence useful in design of storage facilities is the Hurst coefficient, which has been found to have an empirical average near 0.73 for a wide range of geophysical time series (Hurst *et al.*, 1965; Landwehr and Matalas, 1986). The Hurst coefficient for 323-year reconstruction is 0.66, which is below Hurst's empirical average but well above the value of 0.5 expected for a series without long-term persistence. A boxplot-summary of the distribution of Hurst coefficients for 254 overlapping

70-year segments of the reconstruction indicates that the most recent period (1916-1985) provides a biased (high) estimate of long-term persistence (Figure 5). Such bias might be expected given the high-amplitude low-frequency fluctuation in the most recent part of the reconstruction (Figure 3). The reconstruction has virtually the identical Hurst coefficient as the observed flow for the modern period (asterisk and circle in Figure 5). This modern-period value is coincidentally very close to Hurst's (1965) empirical value of 0.73. Most of the coefficients for 70-year segments are below 0.73, but none are as low as 0.5.

### UNCERTAINTY IN THE RECONSTRUCTION

The makeup of the site chronology in the years before the calibration and verification periods bears heavily on the uncertainty of reconstruction. The part of a site chronology used to calibrate and verify the regression equation is assumed to be a representative sample from the same population as the earlier part of the chronology. Changes in sample members (particular trees) and sample size (number of trees) in the chronology over time could invalidate the assumption. Site selection criteria described previously help ensure that the trees in the chronology are limited in growth by the same climatic variables. Adherence to guidelines on subsample signal strength, as discussed previously, helps guard against amplification of noise in the early part of reconstruction due to decreasing sample size.

If the above precautions have been taken in building the chronologies, useful information on accuracy of the entire reconstruction is given by the regression statistics. Confidence bands for reconstructed values are given by the standard error of prediction:

$$SE = \sigma \sqrt{1 + h^*} \tag{2}$$

where  $\sigma$  is the square root of the residual mean square in the calibration period, and  $h^*$  is a multivariate measure of the distance between a given year's predictor data and the mean of the predictor data for the calibration period (Weisberg, 1985). If  $h^*$  for a reconstructed year exceeds the maximum  $h^*$  in the calibration period, the reconstructed value is classified as an extrapolation rather than a prediction, and the error bars defined by  $SE$  might not apply (Weisberg, 1985). By the minimum-covering-ellipsoid approximation (Weisberg, 1985), 16 of the 323 reconstructed values from 1663-1985 were identified as extrapolations. Extrapolations are flagged in the listing of annual reconstructed values (Appendix).

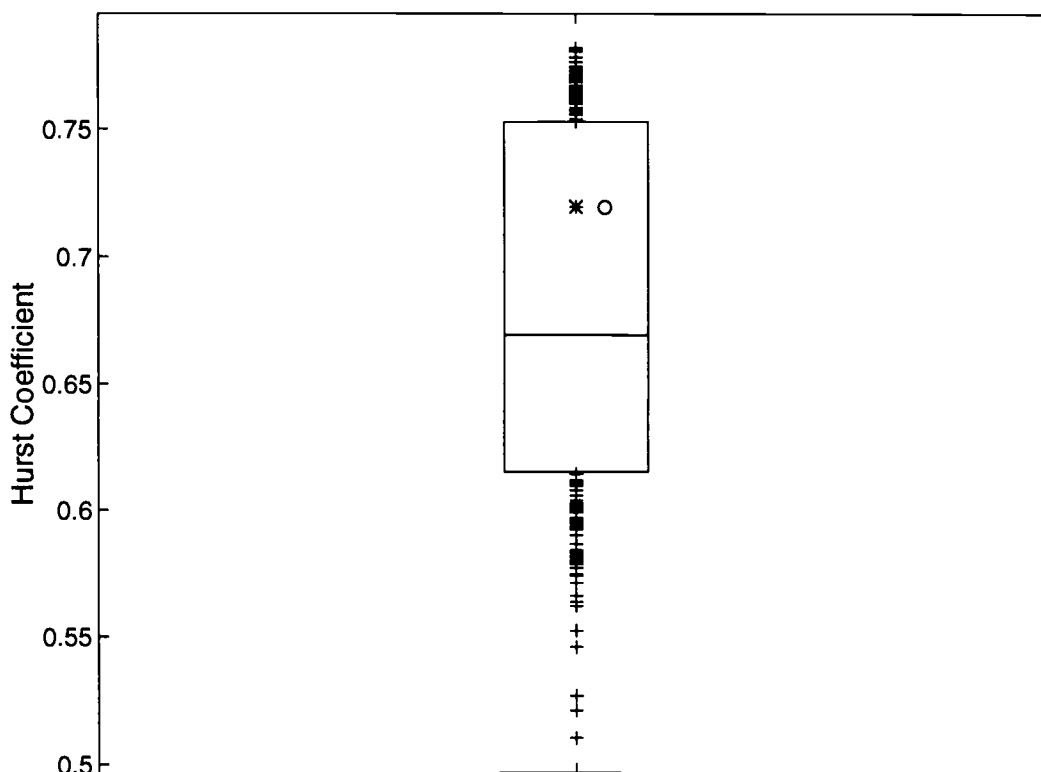


Figure 5. Boxplot Summary of Hurst Coefficient for 254 Overlapping 70-Year Segments of the Gila River Reconstruction. Box delineates 0.25 and 0.75 quantiles; horizontal line marks the median. Observations outside the interquartile range are marked with “+” symbol. Hurst coefficients for most recent period (1916-1985) are marked by the “\*” (reconstruction) and “o” (observed series).

The extremely high reconstructed discharge in the early 1900s should be accepted with caution because six extrapolations occur between 1903 and 1915.

The residual mean square for the reconstruction equation is 0.1876 log acre-ft. The distance measure  $h^*$  varies year by year depending on the distribution of tree-ring data, such that  $SE$  ranges from 0.1908 log acre-ft to 0.2353 log acre-ft. True log-10 discharge theoretically lies within  $\pm 2SE$  of the reconstructed value 95 percent of the time.

Log transformation of discharge before regression has several drawbacks for hydrologic application of reconstructions. Hydrologists typically deal with volume-discharge units (e.g., acre-ft/year), not log-discharge. Reconstructed values can be transformed to acre-ft by taking antilogarithms, but error bars around the transformed values are asymmetrical and are wider for higher discharges than for the lower ones. The two effects are illustrated by error bars for the lowest, highest, and median reconstructed values (Table 5). The confidence band for wet year 1907 spans more than 5 MAF, while the band for dry year 1818 spans only 0.12 MAF.

TABLE 5. Confidence Bands Around Minimum, Median, and Maximum Reconstructed Discharge.

Year <sup>a</sup>	$\hat{y}^b$	se ( $\hat{y}$ ) <sup>c</sup>	Annual Discharge <sup>d</sup> (KAF)		
			Lower	Estimate	Upper
1818	4.6907	.2272	17	49	140
1665	5.4341	.2084	104	272	710
1907	6.3128	.2353	695	2,055	6,074

<sup>a</sup>Years with minimum, median, and maximum values of reconstructed log-10 discharge.

<sup>b</sup>Predicted log-10 discharge.

<sup>c</sup>Standard error of prediction.

<sup>d</sup>“Estimate:” antilogarithm of the reconstructed log-10 discharge. “Lower” and “Upper:” 95 percent prediction interval for transformed log-10 discharge.

A possible alternative to transformation of discharge is to transform the tree-ring data before use in regression. We tried this approach using square-root and other transforms, and found that the regression residuals consistently failed tests for independence from the predictand. Absolute values of residuals typically increased with annual discharge. A difficulty in reconstructing high discharge might be expected

intuitively because additional moisture is unlikely to have a beneficial effect on tree growth once soil moisture levels become extremely high.

## REGIONAL PERSPECTIVE

For a regional perspective on discharge variations, the UGRB reconstruction plotted in Figure 3 was compared with streamflow reconstructions for the Salt and Verde Rivers, which drain the central highlands of Arizona (Smith and Stockton, 1981), and the San Juan River, which derives most of its runoff from mountainous parts of southwestern Colorado (Stockton and Jacoby, 1976).

The UGRB reconstruction correlates significantly with the Salt-Verde ( $r=0.71$ ,  $p\text{-value}<0.01$ ) and San Juan ( $r=0.53$ ,  $p\text{-value}<0.01$ ) reconstructions over the 1663-1969 common period. The dependence of correlation on frequency of variations is given by the squared-coherency between the series (Bloomfield 1976). The squared-coherency plots indicate that the series are significantly correlated at greater than the 99 percent significance level over the full frequency spectrum, with especially high correlation at low frequencies (Figure 6).

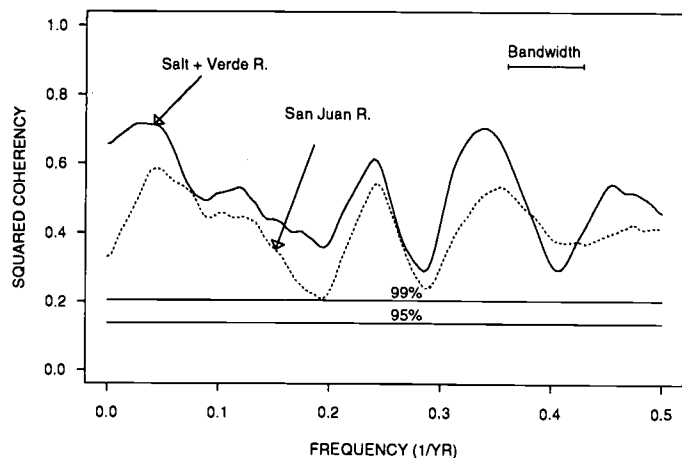


Figure 6. Squared Coherency Between the Gila River Reconstruction and Reconstructions for the Salt and Verde Rivers and San Juan River, 1663-1969. Horizontal lines mark confidence bands.

Low-frequency variations in the three reconstructions were emphasized by smoothing the annual to remove variance at wavelengths shorter than about eight years. The smoothed series are plotted in Figure 7 with horizontal lines at the 0.1 quantile of each

to identify periods of low flow. Troughs in the smoothed UGRB series recur at a rate of about five per century. The amplitude from peak to trough generally exceeds 100 KAF. A similar recurrence interval and amplitude of variation was found for peaks and troughs in 10-year moving averages of the UGRB series (not plotted). Smith and Stockton (1981) reported a 22-year period in the Salt-Verde reconstruction, and Mitchell *et al.* (1979) reported a near-20-year rhythm in tree-ring reconstructed drought-area in the western United States. The spectrum (not shown) of the UGRB series peaks near 20 years, but the recurrence interval of high flows and low flows in the smoothed series is irregular. The interval between minima ranges from 19 years to 29 years from the beginning of record until the 1805 minimum, but later becomes more irregular.

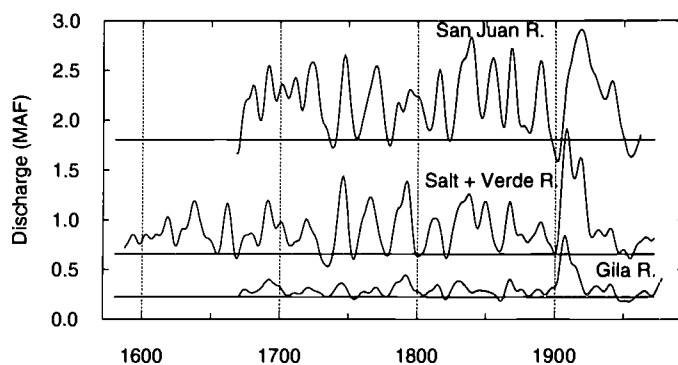


Figure 7. Smoothed Reconstructed Discharge of San Juan, Salt+Verde, and Gila Rivers. Reconstructions for Salt River (annual) and Verde River (October-April total) are after Smith and Stockton (1981); reconstruction for San Juan River is from Stockton and Jacoby (1976). The 0.1 quantile (1670-1972) of each smoothed series is shown by a horizontal line. The quantiles are: 1.805 MAF (million acre-ft) for the San Juan River near Bluff, Utah; 0.656 MAF for the Salt+Verde Rivers at the gages near Roosevelt, Arizona and below Tangle Creek, Arizona; and 0.285 MAF for the Gila River at the head of Safford Valley, Arizona.

Periods of reconstructed low flow generally coincide in the three basins: the eight deepest troughs in UGRB series are matched by troughs in the series for Salt-Verde and San Juan Rivers. The swing from high flow to low flow from the early 1900s to the 1950s is more pronounced in the UGRB than in the San Juan and Salt and Verde basins (Figure 7). All series have low discharge in the 1950s, but only for the UGRB is the 1950s the record minimum in smoothed discharge. Accentuation of the 1950s hydrologic drought over the UGRB is consistent with spatial patterns of seasonal and annual precipitation anomalies (Bradley *et al.*, 1982; Thomas, 1962).

The high-flow period in the early 1900s was also the period of highest spring and summer precipitation since the beginning of instrumental weather records over the UGRB (Bradley *et al.*, 1982). Long gaged discharge records corroborate that discharge during this period was generally high throughout the interior western U.S. (Meko and Stockton, 1984).

### CONCLUDING REMARKS

Tree-ring reconstructions such as those presented can potentially benefit water-resources planning by helping identify periods of the gaged record most suitable for deriving representative long-term water-supply statistics. Reconstructions can also aid in contingency planning by identifying severe hydrologic events within the range of natural variability of the hydrologic system but unrepresented in the period covered by gaged records.

The tree-ring records examined in this paper indicate that large low-frequency variations are characteristic of the discharge history of the Upper Gila River, and that low-frequency variations have been amplified in the 20th century. The clustering of years of high discharge in the early 1900s and low discharge in the 1950s makes the gaged record appear suitable for representing long-term extremes of discharge averaged over several years. The large amplitude of low-frequency variations makes statistics measuring "normal" conditions (e.g., 75-year median annual discharge) sensitive to choice of sample period.

Confidence bands around the reconstruction transformed to acre-ft are much narrower in low-discharge years than in high-discharge years. This reconstruction is therefore best interpreted as a record of drought history. Useful information can be extracted for such features as length and severity of multiyear drought, and exceedance probability of low annual discharge.

Calibration and verification statistics for the Gila River reconstruction are moderately high for tree-ring reconstruction of discharge, but accuracy could possibly be improved by increasing the density of tree-ring coverage through additional collections from the basin. We have restricted our analysis to begin in the 1660s because that is when sample size from living-tree specimens becomes large enough for reliable reconstruction. The time window could possibly be widened many centuries by augmenting data from living trees with data from archaeological and remnant wood specimens.

### ACKNOWLEDGMENTS

We thank Gary Funkhouser and Wanmei Ni, of the Laboratory of Tree-Ring Research at the University of Arizona, for their help in data processing. The research was supported by grants from the United States Bureau of Land Management (Project No. 1422A040C20001 and Cooperative Agreement No. A950-A1-0012), and the National Park Service (Project No. CA801229001).

### LITERATURE CITED

- Anderson, T. W. and N. D. White, 1986. Arizona Surface-Water Resources. *In*: National Water Summary 1985 – Hydrologic Events and Surface-Water Resources. United States Geological Survey Water-Supply Paper 2300, pp. 145-150.
- Box, G. E. P. and G. M. Jenkins, 1976. Time Series Analysis: Forecasting and Control. Holden Day, San Francisco, California, 575 pp.
- Bradley, R. S., R. G. Barry, and G. Kiladis, 1982. Climatic Fluctuations of the Western United States During the Period of Instrumental Records. Contribution No. 42, Department of Geology and Geography, University of Massachusetts, Amherst, Massachusetts, 149 pp.
- Bloomfield, P., 1976. Fourier Analysis of Time Series: An Introduction. John Wiley & Sons, New York, New York, 258 pp.
- Burkham, D. E., 1970. Precipitation, Streamflow, and Major Floods at Selected Sites in the Gila River Drainage Basin Above Coolidge Dam, Arizona. U.S. Geological Survey Professional Paper 655-B, U.S. Government Printing Office, Washington, D.C., 33 pp.
- Cleaveland, M. K. and D. N. Duvick, 1992. Iowa Climate Reconstructed from Tree Rings, 1640-1982. *Water Resources Research* 28(10):2607-2615.
- Cleaveland, M. K. and D. W. Stahle, 1989. Tree Ring Analysis of Surplus and Deficit Runoff in the White River, Arkansas. *Water Resources Research* 25(6):1391-1401.
- Cook, E. R. and L. A. Kairiukstis (Editors), 1990. Methods of Dendrochronology: Applications in the Environmental Sciences. Kluwer Academic Publishers, Boston, Massachusetts, 394 pp.
- Dracup, J. A. and E. Kahya, 1994. The Relationships Between U.S. Streamflow and La Nina Events. *Water Resources Research* 30(7):2133-2141.
- EarthInfo, Inc., 1990. HYDRODATA Users Manual. HYDRODATA, EarthInfo, Inc., 5541 Central Avenue, Boulder, Colorado.
- Fritts, H. C., 1976. Tree Rings and Climate. Academic Press, London, United Kingdom, 567 pp.
- Gold, R. L. and L. P. Denis, 1986. New Mexico Surface-Water Resources. *In*: National Water Summary 1985 – Hydrologic Events and Surface-Water Resources, United States Geological Survey Water-Supply Paper 2300, pp. 341-346.
- Hurst, H. E., R. P. Black, and Y. M. Simaika, 1965. Long-Term Storage: An Experimental Study. Constable & Co. Ltd., London, United Kingdom, 145 pp.
- Landwehr, J. M. and N. C. Matalas, 1986. On the Nature of Persistence in Dendrochronological Records with Implications for Hydrology. *J. of Hydrology* 86:239-277
- Loaiciga, H. A., L. Haston, and J. Michaelsen, 1993. Dendrohydrology and Long-Term Hydrologic Phenomena. *Reviews of Geophysics* 31(2):151-171.
- Meko, D. M. and C. W. Stockton, 1984. Secular Variations in Streamflow in The Western United States. *J. of Climate and Applied Meteorology* 23(6):889-897.
- Mitchell, J. M., Jr., C. W. Stockton, and D. M. Meko, 1979. Evidence of a 22-Year Rhythm of Drought in the Western United States Related to the Hale Solar Cycle Since the 17th Century. *In*: Solar-Terrestrial Influences on Weather and Climate, B. M. McCormac and T. A. Seliga (Editors). D. Reidel Publishing Company, Dordrecht, Holland, pp. 125-143.

- Mosteller, J. and J. W. Tukey, 1977. Data Analysis and Regression: A Second Course in Statistics. Addison-Wesley Publishing Company, Inc., 588 pp.
- Smith, L. P. and C. W. Stockton, 1981. Reconstructed Streamflow for the Salt and Verde Rivers from Tree-Ring Data. Water Resources Bulletin 17(6):939-947.
- Snee, R. D., 1977. Validation of Regression Models: Methods and Examples. Technometrics 19:415-428.
- Stockton, C. W., 1975. Long Term Streamflow Records Reconstructed from Tree Rings. University of Arizona Press, Tucson, Arizona, 111 pp.
- Stockton, C. W. and G. C. Jacoby, 1976. Long-Term Surface-Water Supply and Streamflow Trends in the Upper Colorado River Basin. Lake Powell Research Project Bulletin No. 18, National Science Foundation, 70 pp.
- Thomas, H. E., 1962. The Meteorologic Phenomenon of Drought in the Southwest. U.S. Geological Survey Professional Paper 37A, Washington, Government Printing Office, 43 pp.
- U.S. Army Corps of Engineers, 1971. HEC-4 Monthly Streamflow Simulation, Users Manual. Hydrologic Engineering Center, Corps of Engineers, Department of the Army, Davis, California.
- U.S. Geological Survey, 1970. Surface Water Supply of the United States 1961-65, Part 9, Colorado River Basin; Volume 3, Lower Colorado Basin. Geological Survey Water-Supply Paper 1926, U.S. Government Printing Office, Washington, D.C., 571 pp.
- U.S. Geological Survey, 1980. Water Resources Data for Arizona. U.S. Geological Survey Water-Data Report AZ-79-1, Water Year 1979.
- Weisberg, S., 1985. Applied Linear Regression (Second Edition). John Wiley, New York, New York, 324 pp.
- Wigley, T. M. L., K. R. Briffa, and P. D. Jones, 1984. On the Average Value of Correlated Time Series, with Applications in Dendroclimatology and Hydrometeorology. Journal of Climate and Applied Meteorology 23:201-213.

APPENDIX: RECONSTRUCTED LOG-10 DISCHARGE\*  
(Units: log-10 acre feet)

1663:	5.3098	5.2106	5.4341	5.1801	5.1654	5.1448	5.2039	5.0761	5.5536	5.4165
1673:	5.4987	5.5738	5.5364	5.4532	5.4492	5.3844	5.3111	5.4668	5.3715	5.3897
1683:	5.6080	5.4396	5.0289	5.5791	5.5264	5.5825	5.4598	5.7013	5.3221	5.5587
1693:	5.8903	5.5918	5.5408	5.1501	5.4141	5.5367	5.7410	<u>5.5824</u>	5.5386	5.2551
1703:	5.3643	5.4290	5.3694	5.4450	5.0659	5.4584	5.2323	5.5517	5.4635	5.5466
1713:	5.2669	5.4680	5.2370	5.1632	5.4894	5.5693	5.5098	5.4199	5.6668	5.5187
1723:	5.3942	5.4043	5.4547	5.5702	5.3859	5.1943	<u>5.5815</u>	5.5130	5.3132	5.5046
1733:	5.0080	5.3587	5.2965	5.3472	5.4150	5.4221	5.1597	5.3882	5.7281	5.3254
1743:	5.6623	5.4854	5.4071	5.7125	<u>5.7892</u>	4.9535	5.5317	5.3834	5.5428	5.1036
1753:	5.1603	5.4377	5.1061	5.2670	5.1479	5.4353	5.6263	5.4517	5.0837	5.7012
1763:	5.2452	5.4319	5.3646	5.4726	5.3354	5.3480	5.4461	5.6125	5.8562	5.3746
1773:	4.8000	5.0531	5.5578	5.4051	5.2777	5.3040	5.5288	5.1182	5.2314	5.2106
1783:	5.6649	5.8812	5.4808	5.2779	5.6583	5.2634	<u>5.6767</u>	5.6226	5.7152	5.6028
1793:	5.9928	5.0364	5.3914	5.5854	5.2346	5.1897	5.7345	5.4339	5.1747	5.6432
1803:	5.0604	5.5362	5.2956	5.0351	5.3567	5.5845	5.3913	5.6701	5.3996	5.3654
1813:	5.1823	5.2233	5.7070	<u>5.9932</u>	5.4032	<u>4.6907</u>	5.0917	4.9656	5.4200	5.0701
1823:	5.2434	5.5628	5.5190	5.4671	5.4436	5.6070	5.6470	5.7608	5.4413	5.4388
1833:	5.5912	5.6775	5.7027	5.2178	5.3326	5.4105	5.6181	5.4534	5.1846	5.1877
1843:	5.4720	5.6446	5.5532	5.5449	4.9645	5.2896	<u>5.6428</u>	5.6179	5.1329	5.5397
1853:	5.4419	5.2595	5.4305	5.4780	5.5533	5.3735	5.0737	5.3607	5.1596	5.1395
1863:	4.8940	5.1390	5.5497	5.6993	5.6733	5.8441	5.7147	5.3206	<u>5.1531</u>	5.3648
1873:	5.1722	5.5920	5.5311	5.4029	5.7284	5.4244	5.3581	5.1838	5.0326	5.4673
1883:	5.2934	5.2764	5.6364	5.4830	5.3923	5.4416	5.6475	5.2712	5.6441	5.4259
1893:	<u>5.0054</u>	5.0962	5.3234	5.4101	5.4956	5.9064	5.3646	<u>4.9664</u>	5.4433	4.9667
1903:	<u>5.8392</u>	<u>5.1408</u>	5.6779	<u>6.0545</u>	<u>6.3128</u>	<u>6.0648</u>	5.5023	5.0130	5.6143	5.8979
1913:	5.5607	5.9006	<u>5.8744</u>	5.5164	5.7631	5.1379	5.7506	5.6349	5.2930	5.0426
1923:	5.3249	5.4970	5.0138	5.4689	5.6219	5.5310	5.4553	5.4704	5.7047	5.4648
1933:	5.6208	5.2568	5.4200	5.3139	5.5117	5.4189	5.1499	5.6041	5.9007	5.6120
1943:	5.2536	5.2482	5.3469	5.1618	5.1623	5.2524	5.4998	4.9219	4.9345	5.5570
1953:	5.3558	5.0699	5.0584	4.9389	5.3651	5.4998	5.2998	5.5103	5.1467	5.4286
1963:	5.5257	5.2086	5.4916	5.7275	5.1263	5.5863	5.2026	5.2962	4.8716	5.3893
1973:	5.6956	4.9222	5.5912	5.6013	5.4811	5.4756	5.9393	5.6575	5.3127	5.4388
1983:	5.7190	5.5494	5.6290							

\*Extrapolations underlined.